Applied and Environmental Microbiology, Aug. 2008, p. 4944–4953 Vol. 74, No. 15
0099-2240/08/$08.00+0 doi:10.1128/AEM.00231-08

Expression of Green Fluorescent Protein Fused to Magnetosome Proteins in Microaerophilic Magnetotactic Bacteria▽†

Claus Lang and Dirk Schüler*

Ludwig-Maximillians-Universität München, Department Biologie I, Bereich Mikrobiologie, Maria-Ward-Str. 1a, 80638 Munich, Germany

Received 25 January 2008/Accepted 26 May 2008

The magnetosomes of magnetotactic bacteria are prokaryotic organelles consisting of a magnetite crystal bounded by a phospholipid bilayer that contains a distinct set of proteins with various functions. Because of their unique magnetic and crystalline properties, magnetosome particles are potentially useful as magnetic nanoparticles in a number of applications, which in many cases requires the coupling of functional moieties to the magnetosome membrane. In this work, we studied the use of green fluorescent protein (GFP) as a reporter for the magnetosomal localization and expression of fusion proteins in the microaerophilic *Magnetospirillum gryphiswaldense* by flow cytometry, fluorescence microscopy, and biochemical analysis. Although optimum conditions for high fluorescence and magnetite synthesis were mutually exclusive, we established oxygen-limited growth conditions, which supported growth, magnetite biomineralization, and GFP fluorophore formation at reasonable rates. Under these optimized conditions, we studied the subcellular localization and expression of the GFP-tagged magnetosome proteins MamC, MamF, and MamG by fluorescence microscopy and immunoblotting. While all fusions specifically localized at the magnetosome membrane, MamC-GFP displayed the strongest expression and fluorescence. MamC-GFP-tagged magnetosomes purified from cells displayed strong fluorescence, which was sensitive to detergents but stable under a wide range of temperature and salt concentrations. In summary, our data demonstrate the use of GFP as a reporter for protein localization under magnetite-forming conditions and the utility of MamC as an anchor for magnetosome-specific display of heterologous gene fusions.

The magnetosomes of magnetotactic bacteria are specialized organelles for magnetic orientation that consist of membrane-enveloped crystals of a magnetic iron mineral (1, 34). In strains of *Magnetospirillum*, magnetosomes are synthesized by magnetite (Fe_3O_4) precipitation within specific vesicles formed by the magnetosome membrane (MM), which invaginates from the cytoplasmic membrane and contains a number of specific proteins that are involved in the synthesis of functional magnetosome particles (7, 9, 16, 44). Increasing efforts in interdisciplinary research are aimed at understanding how magnetotactic bacteria achieve their outstanding control over the properties of the magnetic mineral crystals and their assembly into highly ordered chain-like structures (2, 15). Recently, magnetotactic bacteria have emerged as powerful models for the study of cell biology and organelle formation in prokaryotes, as magnetosomes display many common features of eukaryotic organelles (15). In addition, the uniform sizes, crystal habits, and magnetic characteristics of magnetosomes have attracted interest in their use as magnetic nanoparticles with superior properties (20–22), and a number of potential applications, such as magnetic separation and detection of analytes, use as contrast agents in magnetic resonance imaging, or use in magnetic hyperthermia, have been suggested for magnetic nanoparticles derived from magnetic bacteria (13, 24, 52, 55). Many of these applications require the functionalization of isolated magnetosome particles, e.g., by the magnetosome-specific display of functional moieties, such as enzymes, antibody binding proteins, protein tags, or oligonucleotides (22). This has been achieved primarily by chemical coupling of specific ligands to lipids or proteins of the MM (4, 26, 45, 48). Alternatively, the use of integral MM proteins (MMPs) as anchor for the magnetosome-specific display of heterologous proteins fused to them has been suggested (22, 53, 54). For example, luciferase was used as a reporter for the magnetosome expression of genetic fusions to the Mms13 protein of *Magnetospirillum magneticum* (27). Another protein that is useful as a reporter for the expression and intracellular localization of magnetosome proteins is the green fluorescent protein (GFP). The use of GFP fusions has revolutionized the understanding of subcellular organization and membrane targeting in model bacteria, such as *Escherichia coli*, *Bacillus subtilis*, and *Caulobacter crescentus* (25, 41). In addition, GFP has been used as a molecular marker in various environmental microorganisms (23) and has served as a powerful transcriptional reporter to measure real-time gene expression in single living cells by flow cytometry or microscopy (3). GFP-assisted fluorescence microscopy has already been used to study the subcellular localization of several magnetosome proteins in the magnetotactic bacteria *M. magneticum* and *Magnetospirillum gryphiswaldense*. Investigated proteins include the MamA protein, which is presumably involved in the activation of magnetosomes, as well as the acidic MamJ protein and the actin-like MamK protein, both of which control the intracellular assembly of magnetosome chains. Although these examples have demonstrated its principal usefulness in magnetotactic bacteria, the use of GFP as an intracellular marker of magnetosome

* Corresponding author. Mailing address: Ludwig-Maximillians-Universität München, Department Biologie I, Bereich Mikrobiologie, Maria-Ward-Str. 1a, 80638 Munich, Germany. Phone: 498921806145. Fax: 498921806127. E-mail: dirk.schueler@lrz.uni-muenchen.de.

† Supplemental material for this article may be found at http://aem.asm.org/.

▽ Published ahead of print on 6 June 2008.

TABLE 1. Primers used in this study

Primer name	Target gene	Sequence[a]
CL1	*egfp*	**CATATG***GGAGGCGGAGGCGGTGGCGGAG GTGGCGGA*GTGAGCAAGGGCGAGGAG
CL2	*egfp*	GT**GGATCC**TTACTTGTACAGCTCGTC
CL3	*mamG*	**CTCGAG**GGAGATCAGATGATCAAGGG CATC
CL4	*mamG*	**CATATG**AGCAGGCTCGGCGGAGGC
CL5	*mamF*	**CTCGAG**AGGGCAAAGCAATGGCCGAGAC
CL6	*mamF*	**CATATG**GATCAGGGCGACTACATGGCTG
CL7	*mamC*	**CTCGAG**AGGACAACAGCGATGAGCTTTC
CL8	*mamC*	**CATATG**GGCCAATTCTTCCCTCAG

[a] Restriction sites that were incorporated into the primer are indicated in boldface, and the sequence region encoding the glycine-linker is in italics.

TABLE 2. Plasmids used in this study

Plasmid name	Description	Source
pEGFPN-1	GFP expression vector; Ap	BD Biotech
pGEMT-Easy	Cloning vector; Ap	Promega
pCL1	pGEMT-Easy + 10-glycine linker + *egfp*	This study
pCL2	pGEMT-Easy + *mamC*	This study
pCL3	pGEMT-Easy + *mamF*	This study
pCL4	pGEMT-Easy + *mamG*	This study
pBBR1MCS-2	Mobilizable broad-host-range vector; Km	Kovach et al. (18)
pCL5	pBBR1MCS2 + 10G*egfp* from pCL1	This study
pCL6	pCL5 + *mamC* from pCL1	This study
pCL7	pCL5 + *mamF* from pCL2	This study
pCL8	pCL5 + *mamG* from pCL3	This study

localization can be problematic. Magnetite crystals are formed in these microaerophilic organisms only at low oxygen concentrations, below 10^3 Pa (14), while on the other hand, the use of GFP in micro- or anaerobiosis is limited, since the maturation of the protein requires molecular oxygen during the last step of fluorophore maturation (12, 30). Accordingly, it has been noticed that fluorescence intensities and the proportion of fluorescent cells were rather low and varied considerably under microoxic growth conditions, and so far, the application of GFP in relationship to magnetite formation in magnetic bacteria has not been addressed systematically.

This study was intended to investigate the expression of GFP in the microaerophilic *M. gryphiswaldense* at various oxygen levels by flow cytometry and fluorescence microscopy. Cultivation conditions were optimized with respect to growth and biomineralization of magnetite crystals, as well as the maximum expression of GFP and fluorophore formation. We further analyzed by fluorescence microscopy and immunoblotting the subcellular localization of the GFP-tagged magnetosome proteins MamC, MamF, and MamG, which were previously shown to be involved in control of the size of growing magnetite crystals (32). The GFP-modified fluorescent magnetic nanoparticles were purified from bacterial cells, and the stability of expression and fluorescence of MamC-GFP-labeled magnetosomes was studied in vitro under various conditions. These studies served (i) to characterize GFP-modified magnetosomes as a novel biomaterial, which might be useful for biomedical applications, and (ii) as a prerequisite for future experiments using magnetosome proteins as an anchor for the magnetosome-specific display of heterologous gene fusions.

MATERIALS AND METHODS

Strains and growth conditions. *E. coli* strains DH5α and TOP10 (TOP10 chemically competent cells; Invitrogen, Karlsruhe, Germany) were used as hosts for cloning. For conjugation experiments, the *E. coli* strain S17-1 was used (40). *E. coli* strains were grown on Luria-Bertani medium at 37°C; the medium was supplemented with kanamycin or ampicillin (50 μg/ml) if appropriate. Throughout this study, the *M. gryphiswaldense* strain R3/S1, which is a spontaneous rifampin- and streptomycin-resistant mutant of the *M. gryphiswaldense* strain MSR-1, was used (38). *M. gryphiswaldense* was routinely grown microaerobically at 28°C under moderate shaking (100 rpm) in modified FSM medium using 27 mM pyruvate as a carbon source, as described previously (14). For cultivation on petri dishes, agar was added to 1.5% (wt/vol) to FSM medium.

Fermentor production of fluorescent magnetosomes. R3/S1(pCL6) was cultivated in a modified Biostat A Twin dual-vessel laboratory fermentor (B. Braun Biotech International, Melsungen, Germany) in LSM medium as described previously (14). Oxygen electrodes (InPro6000; Mettler Toledo, Gießen, Germany) were calibrated with nitrogen and a microoxic gas mixture (1% oxygen in nitrogen) or synthetic air (flow rate, 3 liters min^{-1}) as described by Heyen and Schüler (14). The medium (10 liters) was inoculated with a 1-liter preculture grown in a 2-liter flask containing air in the headspace. The fermentor was inoculated to an initial cell density of approximately 1×10^7 cells ml^{-1}. During cultivation agitation (150 rpm), the temperature (28°C) and pH (7.0) were maintained constant. Bacteria were grown microaerobically at 12.5 or 200 Pa oxygen until stationary phase for 24 h. Alternatively, the bacteria were cultivated aerobically at 2×10^4 Pa oxygen for 16 h and subsequently shifted to 20 Pa, as indicated in the experiments.

Molecular genetic techniques. If not otherwise specified, standard DNA procedures were employed (31). Cloned genes and fusion constructs were sequenced using BigDye terminator v3.1 chemistry on an ABI 3700 capillary sequencer (Applied Biosystems, Darmstadt, Germany). Sequence data were analyzed with Lasergene 6 (DNAstar Inc., Madison, WI). Primers were purchased from Carl Roth GmbH (Karlsruhe, Germany) and MWG Biotech (Ebersberg, Germany). The primer sequences are listed in Table 1.

Construction of GFP fusion proteins. In this study, the GFPmut1 variant, which is also termed EGFP (enhanced GFP), was used (5, 23). The *egfp* gene was PCR amplified (Taq-Mastermix; Promega, Heidelberg, Germany) from the pEGFPN-1 (BD Biotech) plasmid using the CL1 forward primer, which adds an NdeI restriction site and a 10-glycine linker to the 5′ end of the *egfp* gene, and reverse primer CL2. The PCR product was cloned into pGEMT-Easy (Promega) to yield pCL1. The *mamC* (CL7 and CL8), *mamF* (CL5 and CL6), and *mamG* (CL3 and CL4) genes were amplified with the corresponding primer pairs (in parentheses) using genomic DNA of *M. gryphiswaldense* R3/S1 as a template. The PCR products were cloned into pGEMT-Easy (Promega) and transformed into $CaCl_2$-competent DH5α to generate pCL2-4. The *egfp* gene was subcloned from pCL1 into the EcoRI site of the pBBR1MCS-2 (18) plasmid to yield the plasmid pCL5. Colony PCR was performed to screen for plasmids in which *egfp* was present in the same orientation as the *lac* promoter. Translational fusions of *mamC*, *mamF*, and *mamG* with *egfp* connected via a 10-glycine linker were constructed by ligating the respective *mam* genes from pCL2, pCL3, and pCL4 into the NdeI and XhoI sites of the pCL5 vector to generate the plasmids pCL6, pCL7, and pCL8, respectively. For a complete list of the plasmids used in this study, refer to Table 2. The plasmids harboring the *mam-egfp* fusions were transferred into *M. gryphiswaldense* R3/S1 by conjugation from *E. coli* S17-1, as described previously (39).

Fluorescence microscopy. *M. gryphiswaldense* strains R3/S1 bearing the plasmids pCL5 to pCL8 were grown in 15 ml polypropylene tubes with sealed screw caps and a culture volume of 11 ml to stationary phase. The cell membranes were stained with the membrane stain FM4-64 (Invitrogen, Karlsruhe, Germany) at a final concentration of 1.5 μM. The stained cells were immobilized on agarose pads (FSM medium excluding yeast extract and peptone but supplemented with 1% agarose). The immobilized cells were imaged with an Olympus BX61 microscope equipped with a 100× UPLSAPO100XO objective with a numerical aperture of 1.40 and an Olympus F-View II camera. Images were captured and analyzed using Olympus cell and ImageJ 1.36b software. For the microscopic visualization of fluorescent magnetosomes, approximately 15 μl of a magnetosome suspension with a magnetosome concentration corresponding to an iron concentration of 10 mM was spotted on a microscope slide. After placement of

a bar magnet next to the microscope slide, the fluorescent magnetosomes were imaged with a Zeiss LSM510 microscope equipped with a 10× objective and a Photometrics Coolsnap HQ camera.

Analytical procedures. Cell growth and magnetism were measured turbidimetrically at 565 nm. The average magnetic orientation of cell suspensions was assayed as previously described (36). Briefly, an external magnetic field was employed to align the cells at different angles relative to the light beam. The ratio of the resulting maximum and minimum extinction (C_{mag}) is correlated with the average number of magnetic particles per cell and was used as a semiquantitative assessment of magnetite formation (a C_{mag} of 0 was assumed for nonmagnetic cells).

For the determination of the iron concentration of magnetosome suspensions, magnetosomes were sedimented by centrifugation, resuspended in 65% HNO_3, and incubated at 99°C overnight to dissolve the magnetite crystals. The iron content of the solution was determined with a modified version (47) of the ferrozine assay (42).

The protein concentrations of the cell lysate (CL) and the nonmagnetic (NF), soluble (SP), membranous (MP), and magnetosome protein fractions were assessed with a bicinchoninic protein quantification kit (Sigma, Munich, Germany) according to the manufacturer's instructions.

The magnetosome bound fluorescence was quantified with an Infinite 500 96-well fluorescence reader using I-Control v1.2.7.0 software (Tecan, Crailsheim, Germany). The excitation wavelength was 485 nm (20-nm bandwidth), and emission was recorded at 535 nm (25-nm bandwidth). Different dilutions of magnetosomes (0 to 10 mM iron) were prepared in triplicate in 100 μl EP (10 mM HEPES, 1 mM EDTA, pH 7.4) in a black 96-well Nunclon plate. The value for each sample was averaged from 10 reads over an integration period of 20 μs.

Flow cytometry. Flow cytometry was performed with a FACScalibur flow cytometer (Becton-Dickinson) equipped with an argon laser emitting at 488 nm. GFP fluorescence was recorded in the FL-1 channel. Cells of *M. gryphiswaldense* R3/S1 and derivatives bearing the plasmids pCL5 to pCL8 were washed in phosphate-buffered saline and resuspended in phosphate-buffered saline at a 1:100 dilution to maintain a counting speed between 300 and 1,000 events s^{-1}. Unless otherwise indicated, 50,000 events were counted. The data were analyzed using FlowJo software (Treestar). Untransformed R3/S1 was used as a nonfluorescent standard. Contaminating cell debris and medium constituents were excluded from the analysis based on forward and side scatter data. To estimate the proportion of fluorescent cells, a threshold for fluorescence was set to the fluorescence intensity below which 99% of untransformed R3/S1 cells were detected.

Isolation of magnetosomes. The procedure for magnetosome purification was modified from that of Grünberg et al. (9). *M. gryphiswaldense* strains were exposed to air in sealed 5-liter flasks (Schott, Mainz, Germany) containing 4 liters modified FSM medium. The cultures were inoculated with 400 ml overnight culture to a cell density of approximately 1×10^7 cells ml^{-1}. The cultures were incubated at 28°C with moderate shaking (120 rpm). Stationary-phase cultures were harvested by centrifugation, washed with WB (20 mM HEPES, 1 mM EDTA, pH 7.4), and finally resuspended in RB (50 mM HEPES, 1 mM EDTA, 0.1 mM phenylmethylsulfonyl fluoride, pH 7.4). The cells were disrupted by three passages through a French press at 1.26×10^8 Pa. Cell debris was removed by centrifugation at 800 × *g* for 5 min. The cleared CL was passed through a MACS magnetic-separation column placed between Sm-Co magnets (Miltenyi, Bergisch Gladbach, Germany) to separate magnetosomes from the NF. The column bound magnetosomes were washed with 10 column volumes (50 ml) of EP, HP (10 mM HEPES, 200 mM NaCl, 1 mM EDTA, pH 7.4), and water before the magnetic field was removed and the magnetosomes were eluted in EP. Subsequently, the magnetosomes were centrifuged through an 8-ml sucrose cushion (60% [wt/wt] in EP) at 200,000 × *g* for 90 min. Due to their high specific density, magnetosomes sediment at the bottom of the tube, whereas other cellular constituents are retained by the sucrose cushion. Finally, the magnetosomes were resuspended in 2 ml EP.

The NF, which was not retained by the magnetic column, was subjected to centrifugation at 4,000 × *g* for 60 min to remove residual cell debris. The supernatant was subjected to 2 h of centrifugation at 100,000 × *g* to separate the cellular membranes from the SP. The sedimented membrane fraction was resuspended in EP and centrifuged a second time at 100,000 × *g* for 2 h. The membrane proteins were resuspended in EP supplemented with 1% sodium dodecyl sulfate (SDS).

SDS-PAGE and Western blot analysis. Polyacrylamide gels were prepared according to the procedure of Laemmli (19). Protein samples from different cellular fractions were resuspended in electrophoresis sample buffer (62.5 mM Tris-HCl, pH 6.8, 0.1 M dithiothreitol, 1.6% SDS, 5% glycerol, 0.002% bromophenol blue) and denatured at 100°C for 5 min. Fifteen micrograms of protein was loaded onto the gels. For SDS-polyacrylamide gel electrophoresis (PAGE) analysis of the relative abundances of fusion proteins present in the MM, MMPs were separated on 15% (wt/vol) gels and proteins were visualized by Coomassie brilliant blue staining. For Western blot analysis, 10% (wt/vol) gels were used, and following electrophoresis, proteins were transferred onto nitrocellulose membranes (Protran; Whatman, Germany) by electroblotting. The membranes were blocked for 2 h at room temperature. An anti-GFP antibody (Santa Cruz, Biotechnology, Inc.) or an anti-MamC antibody (8) was added to the blocking solution at 1:1,000 or 1:500 dilution, respectively, and the mixture was incubated for 1 h at room temperature. The membrane was washed several times with Tween–Tris-buffered saline and Tris-buffered saline (TBS) before alkaline phosphatase-labeled goat anti-rabbit immunoglobulin G antibody (Santa Cruz, Biotechnology, Inc.) was added at 1:1,000 dilution in TBS. After incubation at room temperature for 45 min, the membrane was washed with TBS, and the BCIP (5-bromo-4-chloro-3-indolylphosphate)/nitroblue tetrazolium detection reagent (Roche Diagnostics, Mannheim, Germany) was used for detection.

Stability assays of magnetosome fluorescence. A stock solution with a defined magnetosome concentration (2 mM iron) was prepared in EP and dispensed in 100-μl portions into 1.5-ml reaction tubes. The magnetosomes were magnetically separated for 2 minutes by attaching a neodymium magnet to the side of the tube. The supernatant was aspirated, and the magnetosomes were resuspended in 100 μl of a buffer containing the desired constitution. For pH testing, buffer S (40 mM boric acid, 40 mM phosphoric acid) was adjusted with sodium hydroxide to values of pH 3 to pH 11 (51). Stability to detergents was tested by resuspending the magnetosomes in buffer S (pH 8) containing different SDS or Triton X-100 concentrations from 0 to 1% (wt/vol). To investigate the effect of guanidinium chloride, the magnetosomes were resuspended in buffer S (pH 8) containing between 0 and 1 M guanidinium chloride. The influence of sodium chloride was tested with buffer S (pH 8) supplemented with 0, 0.1, 0.5, 1, 2, and 4 M sodium chloride. After the magnetosome suspensions were incubated for 1 h at 4°C, the magnetosomes were separated magnetically as described above and resuspended in buffer S (pH 8), and the fluorescence was quantified with a fluorescence reader. The influence of the storage temperature was tested by incubating the magnetosome suspensions in buffer S (pH 8) at temperatures between −20 and 70°C for 12 h, followed by magnetic separation, resuspension in the same buffer, and fluorescence quantification as described above.

RESULTS

Optimization of growth conditions for maximum GFP fluorophore formation and magnetite synthesis. Synthesis of magnetite crystals in *M. gryphiswaldense* occurs only below an oxygen partial pressure of 1.0×10^3 Pa (14, 35, 50). In initial experiments, we noticed that under these microoxic conditions, only a small and highly variable proportion of cells expressing GFP were fluorescent, and the emitted signal was rather weak and varied between different growth experiments (C. Lang and D. Schüler, unpublished observation). As we reasoned that poor GFP fluorescence expression was due to limited availability of oxygen for fluorophore biosynthesis, we performed a number of experiments in order to establish growth conditions that would provide both strong GFP expression and magnetite biomineralization. First, cells expressing GFP from the *lac* promoter on pCL5 were grown in sealed batch flask cultures with various headspace-to-volume ratios and under different headspace oxygen concentrations. As shown in Table 3 the proportion of fluorescent cells and magnetic orientation (as monitored by the C_{mag}) displayed an inverse dependence on the aeration. For example, under standard cultivation conditions (1% oxygen in the culture headspace), which were used for maximal magnetite production, only 8.5% of the cells displayed significant fluorescence. The highest proportion of fluorescent cells (~22%) was found at the highest aeration of 21% oxygen in the headspace. However, cells were completely devoid of magnetite crystals ($C_{mag} = 0$) under these conditions. The proportion of fluorescent cells and the average in-

TABLE 3. Flow cytometric analyses of different GFP- and GFP fusion-expressing derivatives of *M. gryphiswaldense* cultivated under different conditions

Strain	Culture conditions	Growth stage[a]	Magnetism (C_{mag})	Avg fluorescence	Cell proportion above threshold (%)
M. gryphiswaldense(pCL5)	1% oxygen; 100-ml culture in 1-liter flask	0.095	1.7	18.1	8.5
	10% oxygen; 100-ml culture in 1-liter flask	0.183	1.5	41.9	20.0
	21% oxygen; 100-ml culture in 1-liter flask	0.138	0.0	52.3	20.4
	21% oxygen; 100-ml culture in 500-ml flask	0.224	0.0	50.1	22
	21% oxygen; 400-ml culture in 500-ml flask	0.220	1.7	42.6	19.7
	21% oxygen; 4-liter culture in 5-liter flask	0.408	2.0	30.8	22.3
M. gryphiswaldense(pCL6)	21% oxygen; 4-liter culture in 5-liter flask	0.532	1.9	42	22
	12 Pa oxygen; 10-liter fermentor	0.624	1.3	22.8	10.8
	200 Pa oxygen; 10-liter fermentor	0.540	1.6	27.8	15.8
	2×10^4 Pa oxygen; 10-liter fermentor	0.480	0.2	46.2	26.1
	2×10^4 Pa oxygen for 16 h + 20 Pa for 8 h; 10-liter fermentor	0.624	1.3	42.4	20.3
M. gryphiswaldense(pCL7)	21% oxygen; 4-liter culture in 5-liter flask	0.408	1.7	15.6	5.3
M. gryphiswaldense(pCL8)	21% oxygen; 4-liter culture in 5-liter flask	0.416	1.5	24.9	17

[a] Optical density at 565 nm.

tensity increased with the oxygen availability, and both magnetite formation and fluorescence intensity were reasonably high if the headspace-to-liquid ratio was approximately 1:4 and air was used in the headspace (Table 3). Next, we investigated the fluorescence of GFP fused to the MMPs MamG, MamC, and MamF under these optimized conditions. The expression and intracellular localization of these three proteins were of primary interest, as they represent the most abundant proteins in the MM and are tightly bound to the magnetosome by several transmembrane domains and thus are promising candidates for anchors to display fusion proteins on the surfaces of magnetosome particles (9, 32). As with unfused GFP, cultures expressing GFP fused to MamC, MamF, and MamG, from the plasmids pCL6, pCL7, and pCL8, respectively, displayed reasonable magnetite formation and high fluorescence, and large proportions of fluorescent cells were obtained in flask cultures grown under the optimized conditions described above. However, the fusions displayed different fluorescence intensities, and the highest fluorescence was observed with MamC-GFP, followed by MamF-GFP and MamG-GFP (Fig. 1 and Table 3).

In summary, the best compromise with respect to magnetite formation and GFP fluorescence was obtained in flask cultures with a growth-limiting oxygen supply, in which oxygen concentrations declined from high initial levels in the medium with increasing cell numbers, eventually reaching low dissolved oxygen concentrations, permitting magnetite synthesis (14, 35). As this was accompanied by a change in conditions during growth, further experiments were performed in an oxystat fermentor, which allowed the precise maintenance of a constant oxygen partial pressure over the entire incubation period (14). Cells expressing MamC-GFP from pCL6 were highly magnetic at 12 Pa oxygen; however, only 10.8% of the R3/S1(pCL6) cells exhibited fluorescence levels above that of the untransformed control. On the other hand, the fluorescence intensities and proportions of fluorescent cells (26.1%) were highest at an oxygen partial pressure of 2×10^4 Pa, which, however, entirely repressed magnetite synthesis. At an intermediate oxygen partial pressure of 2×10^2 Pa, the culture produced magnetite,

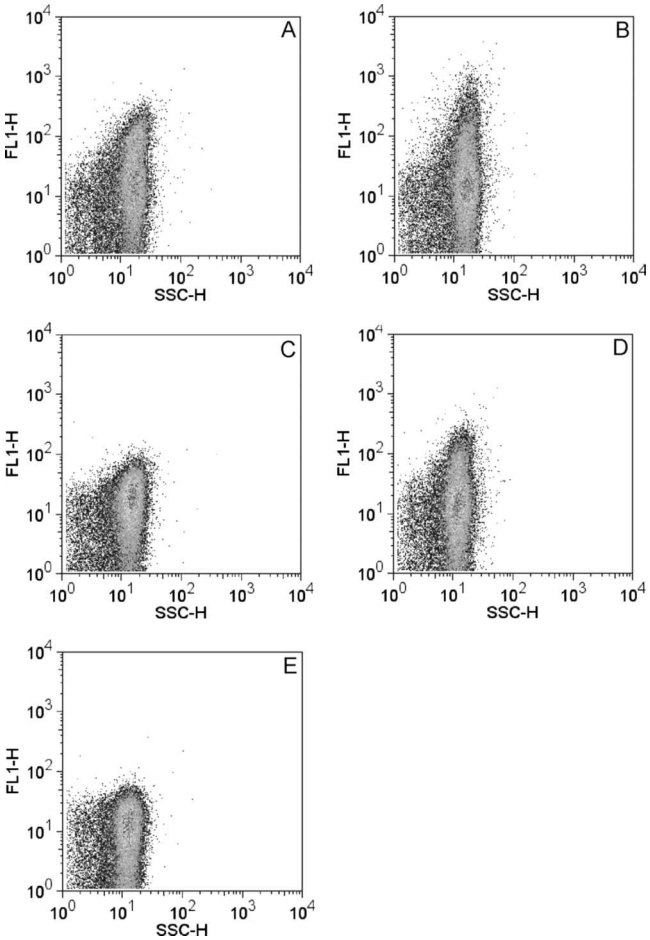

FIG. 1. (A to D) Flow cytometric analysis of *M. gryphiswaldense* R3/S1 expressing either GFP (pCL5) (A), MamC-GFP (pCL6) (B), MamG-GFP (pCL8) (C), or MamF-GFP (pCL7) (D). (E) Analysis of the untransformed *M. gryphiswaldense* strain. The fluorescence intensity (FL1-H) of each event was plotted against the side scatter (SSC).

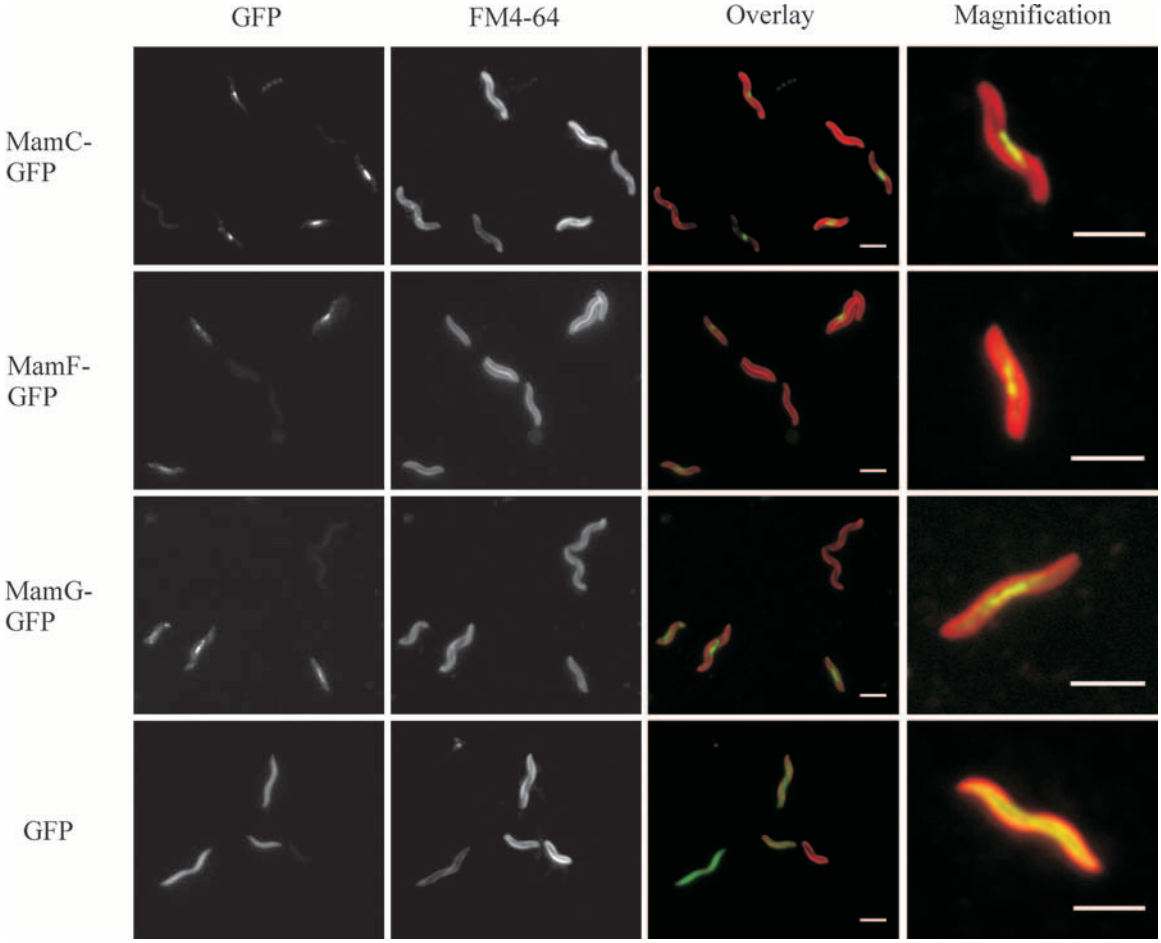

FIG. 2. Fluorescence micrographs of *M. gryphiswaldense* strain R3/S1 expressing MamC-GFP (pCL6), MamF-GFP (pCL7), MamG-GFP (pCL8), or GFP (pCL5). In the first column, the GFP fluorescence signals are shown. In the second column, the signals of the membrane stain FM4-64 are shown for the same cells displayed in the first column, and in the third column, the overlays of the GFP (green) and FM4-64 (red) signals are displayed. The fourth column shows an enlargement of an overlay of a single representative cell. Scale bars, 3 μm.

but only 15.8% of the cells were fluorescent, and the average fluorescence was low, with an intensity only 22% higher than that of the culture grown at 1.2×10^3 Pa oxygen (Table 3).

As we concluded from these experiments that strong fluorescence and maximum magnetite synthesis are mutually exclusive at any constant oxygen level, shift experiments were performed, in which the cells were initially grown for 16 h under fully oxic conditions (2×10^4 Pa) to an optical density at 565 nm of 0.310 and then shifted to microoxic conditions (20 Pa) for 8 hours. This treatment resulted in a magnetic culture with 20.3% fluorescent cells and a fluorescence intensity that had increased by 50% compared to the microoxically grown culture (Table 3). In addition, we attempted first to incubate the bacteria under microoxic conditions and subsequently to induce GFP maturation by exposure to air. However, these experiments were unsuccessful, as the fluorescence did not increase over an incubation period of 6 h and the cells ceased growth after the shift (data not shown).

The GFP fusions to MamC, MamF, and MamG are specifically expressed in the MM. (i) In vivo localization of GFP fusions of MamC, MamF, and MamG. Next, we studied the expression and subcellular localization of GFP fusions of the GFP-tagged MamC, MamF, and MamG proteins by fluorescence microscopy under conditions of magnetite formation. In cells expressing MamC-GFP, MamF-GFP, and MamG-GFP, the fluorescence was typically observed as linear signals along the cell axis at midcell, where the magnetosome chain is usually located (Fig. 2). With all three fusions, the signals appeared either predominantly as 0.5 to 2 μm straight lines or, less frequently, as punctuated lines. The linear signals were observed either at the concave side of the cells or at the shortest connection from one turn to the next, which is consistent with a localization along the axis of the twist of the helical cells. In MamC-GFP-expressing cells, the signal was occasionally observed as a single bright fluorescent spot at midcell. No significant fluorescence was associated with the cytoplasmic membrane for any of the fusions. However, some fluorescence was detectable in the cytoplasm of cells expressing MamF-GFP and MamG-GFP (approximately 100% and 50% above the background fluorescence of the medium), whereas the MamC-GFP fusions displayed almost no cytoplasmic fluorescence (<10% above background). Control cells expressing unfused GFP displayed fluorescence evenly distributed over the cytoplasm (Fig. 2).

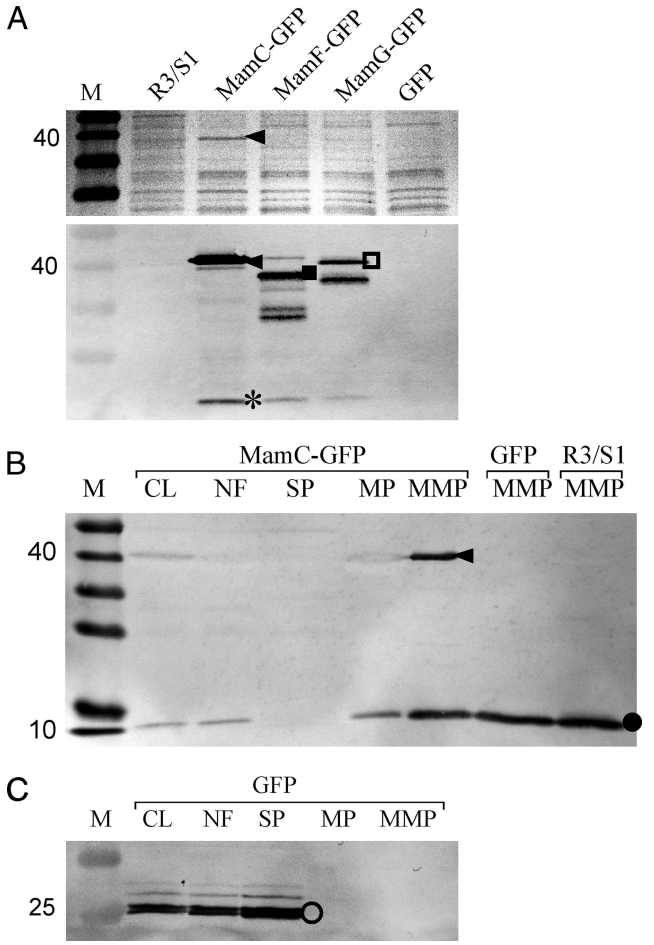

FIG. 3. Detection of GFP fusion proteins in isolated magnetosomes and other cell fractions. M, marker. (A) Detection of GFP fusion proteins on isolated magnetosomes. (Top) SDS-PAGE of purified MMPs from the *M. gryphiswaldense* R3/S1 strain and derivatives harboring the plasmids pCL5 (GFP), pCL6 (MamC-GFP), pCL7 (MamF-GFP), and pCL8 (MamG-GFP). The MamC-GFP signal is indicated by an arrowhead. (Bottom) Immunoblot of a gel identical to that shown at the top probed with an anti-GFP antibody. Besides the MamC-GFP signal (arrowhead), signals for MamF-GFP (■) and MamG-GFP (□) are shown. In addition, a putatively nonspecific signal (*) was detected at a mass of 20 kDa in the magnetosome fractions of MamC-GFP-, MamF-GFP-, and MamG-GFP-expressing cells. (B) Immundetection of MamC (●) and MamC-GFP (arrowhead) in different cell fractions of R3/S1(pCL6) (MamC-GFP) and in the MM fractions of R3/S1(pCL5) (GFP) and R3/S1 with an anti-MamC antibody. (C) Immunodetection of GFP (○) in different cell fractions of R3/S1(pCL5) (GFP) with an anti-GFP antibody.

(ii) Immunoblot analysis of MamC-, MamF-, and MamG-GFP localization. The localization and expression of GFP fusions were further studied by SDS-PAGE and immunodetection in cell fractions prepared from fluorescent and magnetic cells. An additional protein band of the expected mass of the MamC-GFP fusion protein (40 kDa) was detected by Coomassie staining in magnetosomes from cells expressing MamC-GFP (Fig. 3A, top). Bands corresponding to MamF-GFP (40.1 kDa) and MamG-GFP (35.5 kDa) were below the detection level by Coomassie (Fig. 3A, top) but were recognized with an anti-GFP antibody (Fig. 3A, bottom). In addition, a band of roughly 20 kDa was immunodetected in the magnetosome fractions from all three of the GFP fusions, and further bands representing products of proteolytic cleavage were visible in MM preparations from MamF-GFP and MamG-GFP, indicating that these fusions were partially degraded in the cells (Fig. 3A, bottom).

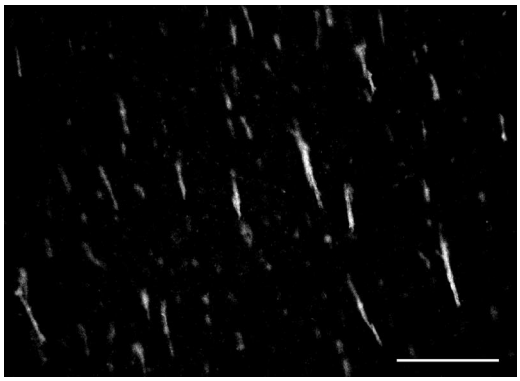

FIG. 4. Fluorescence micrographs of magnetosome particles isolated from R3/S1 (pCL6). The magnetosome particles aggregated into bundles of chains in the presence of an ambient magnetic field. Scale bar, 100 μm.

Immunodetection of the MamC-GFP fusion by an anti-MamC antibody revealed the strongest signal in the MMP fraction, whereas a weak band of this size was also recognized in the NF, the MP, and the CL, but not the SP (Fig. 3B). Native, unfused MamC recognized by anti-MamC as a band of 12.5 kDa displayed a subcellular distribution identical to that of MamC-GFP. The presence of low levels of MamC and MamC-GFP in the NF and the MP was probably caused by MMs that evaded the magnetic-separation procedure, such as empty magnetosome vesicles, vesicles containing immature magnetite crystals, and MMs that were detached during the purification procedure. The intensity of the MamC-GFP band was approximately 80% of that of the MamC band, indicating that the fusion and the native protein are expressed in comparable quantities (Fig. 3B). MamF-GFP and MamG-GFP were exclusively detected as weak bands only in the MMP fraction but were below detection in other subcellular fractions, including the entire CL (data not shown), which indicates that MamF-GFP and MamG-GFP are present only in small amounts, due to either strong degradation or poor expression. For comparison, unfused GFP was recognized by an anti-GFP antibody at the expected mass of approximately 27 kDa in the CL, the NF, and the SP, but not in the MP or the MMP (Fig. 3C).

Isolated magnetosomes expressing GFP fusions to MamC, MamF, and MamG display stable fluorescence in vitro. The next question was whether GFP fusions expressed on magnetosomes retain functionality in vitro, as in vitro stability would be a prerequisite for any future application of protein genetically fused to magnetosome proteins. Freshly isolated magnetosomes expressing MamC-GFP, MamF-GFP, or MamG-GFP displayed strong fluorescence, which was visible under the fluorescence microscope in the form of bundles of chains that formed in the presence of an ambient magnetic field (Fig. 4; also see the supplemental material). MamC-GFP magneto-

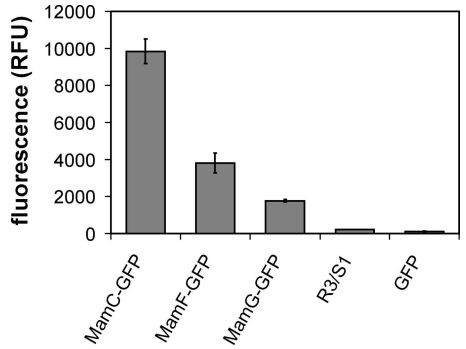

FIG. 5. Fluorescene measurements of magnetosomes isolated from the R3/S1 strain or R3/S1 derivatives harboring the plasmids pCL5 (GFP), pCL6 (MamC-GFP), pCL7 (MamF-GFP), and pCL8 (MamG-GFP). Fluorescence was quantified on 100-μl aliquots of magnetosome suspensions containing a magnetosome amount equivalent to 5 mM iron. RFU, relative fluorescence units.

somes displayed the highest fluorescence, while the fluorescences of MamF-GFP and MamG-GFP magnetosomes of cells from identical cultures were approximately threefold (MamF-GFP) and fivefold (MamG-GFP) lower (Fig. 5). The stabilities of fluorescent magnetosomes were tested by measuring the fluorescence after incubation under various conditions, including different pHs, temperatures, and salt and detergent concentrations (Fig. 6). The highest fluorescence intensity was retained between pH 8 and pH 9, which is close to the reported optimum pH of GFP (29), and at pH 11, the intensity was still 20% of the value at pH 9, whereas fluorescence was abolished at acidic pH, below pH 6. At pH 7, only 60% of the intensity was retained. The fluorescence intensity was equally high if magnetosomes were stored at temperatures below 24°C or frozen at −20°C. A temperature increase to 30°C or 50°C led to a decrease (~20%) in fluorescence, and after storage at 70°C, only approximately 15% of the fluorescence of magnetosomes stored at 4°C was retained. In addition, the particles incubated at this high temperature rapidly agglomerated, indicating that the membrane enclosing the particles became disturbed, probably due to denaturation. Sodium chloride had a quenching effect on the magnetosome fluorescence only at a high concentration of 4 M, and guanidinium chloride reduced the fluorescence intensity to roughly 50% at a concentration of 1 M. However, the detergents SDS and Triton X-100 led to a loss of approximately 80% of the magnetosome bound fluorescence at a concentration of 0.05%, probably due to solubilization and loss of MamC-GFP. Remarkably, a fluorescence of approximately 20% was retained even at higher detergent concentrations, which might be due to nonspecific adsorption of MamC-GFP to the surfaces of magnetite crystals after membrane solubilization.

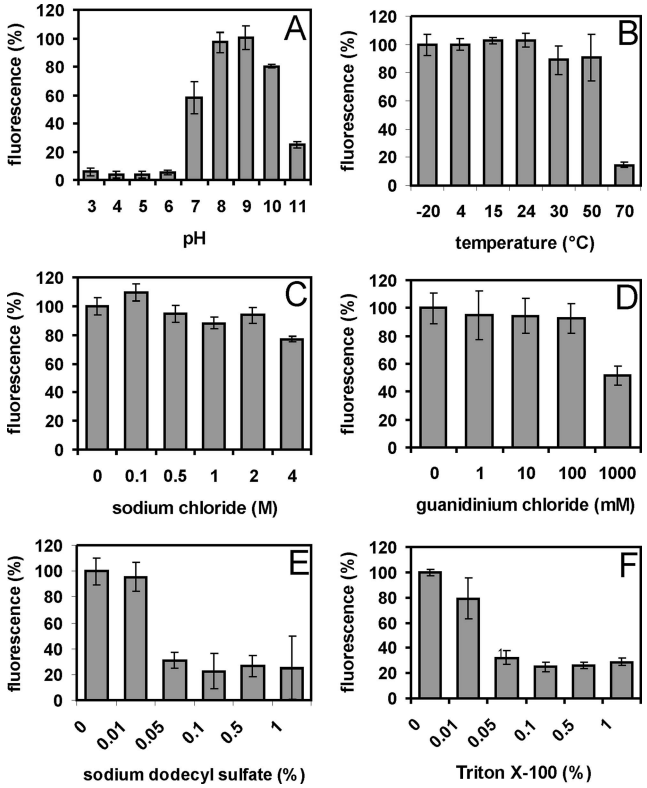

FIG. 6. In vitro stability of fluorescent magnetosomes purified from R3/S1(pCL6). (A) Effect of pH of the buffer on magnetosome fluorescence. (B) Thermal stability of the magnetosome bound fluorescence. (C to F) Fluorescences of magnetosomes incubated with different amounts of sodium chloride (C), guanidinium chloride (D), SDS (E), or triton X-100 (F). Following an incubation period of 1 hour, the magnetosomes were magnetically separated and resuspended in buffer S, pH 8, to remove unbound fluorophores. Subsequently, the stability of the magnetosomes was assessed by fluorescence quantification. The error bars represent the standard deviations, which were calculated from four independent experiments.

DISCUSSION

Although GFP has been used previously as a tag to follow the subcellular localization of magnetosome proteins in microaerophilic magnetotactic bacteria (16, 17, 33, 37), its expression and activity under the microoxic conditions required for magnetite synthesis have not yet been assessed systematically. However, they are crucial for correlating protein localization with the positions of magnetite crystals and chains. Here, we have demonstrated that the optimum conditions for fluorophore formation and magnetite synthesis are mutually exclusive, and no permanent growth condition was found to permit high fluorescence and magnetite synthesis simultaneously. Magnetite synthesis occurs only below 1×10^3 Pa (14), whereas GFP requires molecular oxygen during fluorophore maturation, which limits its use in oxygen-limited systems (30). This problem has been partially overcome in a variety of anaerobic and microaerophilic bacteria by shifting anaerobically grown cells to oxic conditions after growth to stimulate fluorophore formation. For example, in *Enterobacter aerogenes*, a 60-min shift from anaerobic to aerobic conditions was sufficient to double fluorescence (56). Hansen et al. found that the GFP variant GFPmut3* displayed fluorescence in *Streptococcus gordonii* with 0.1 ppm dissolved oxygen. In the same study, it was also observed that fluorescence was activated in an anaerobically grown, nonfluorescent *S. gordonii* biofilm by a 20-min shift to aerobic conditions (11). In anaerobically grown *Rhodobacter sphaeroides*, GFP was visualized after 4 h of aeration by vigorous shaking (49). An abrupt shift from anoxic or

microoxic conditions to oxic conditions did not induce fluorophore formation in *M. gryphiswaldense* in our experiments, but it inhibited further growth. The highest percentages of both fluorescent and magnetic cells were obtained, when fluorophore formation and magnetite synthesis became sequentially induced, if culture conditions were chosen that provided gradually decreasing oxygen levels during the incubation due to the increasing oxygen consumption of cells. Although the proportion of fluorescent cells never reached 100%, nearly all cells under these conditions contained magnetosome chains (data not shown). Our data also show that even under high oxygen tensions, only 22 to 26% of the cells displayed significant fluorescence intensities. This may be attributed to a low expression level of GFP from the *lac* promoter. In addition, dependence of protein expression on the cell cycle within a heterogeneous population and stochasticity of gene expression might be involved, as described for other bacteria (6, 43).

Of all tested fusions, the MamC-GFP fusion displayed the highest fluorescence both in vivo and on isolated magnetosomes, which was consistent with the highest abundance of both the fusion and the unfused MamC protein, which displayed similar expression levels. In contrast, MamF-GFP and MamG-GFP fusions were below the detection level by Coomassie in MM preparations. The immunodetection of several proteolytic degradation products of MamF- and MamG-GFP fusions indicated that these proteins are less stable. GFP fusions to MamF and MamG were substantially more weakly expressed than their unfused counterparts. This could be explained either by a bias in targeting to the MM or by relatively low expression from the *lac* promoter present on the vector backbone, which makes future expression studies of native or inducible promoters highly desirable.

The GFP fusions of MamC, MamF, and MamG displayed nearly identical localization patterns, and the extension of the linear fluorescence signal correlated well with the typical length and position of the magnetosome chain. The results of localization studies are in agreement with previous biochemical studies (9) and with the immunogold labeling studies of Mam12, which is orthologous to MamC in *M. magnetotacticum.* However, due to the weak immunogold signals, the immunogold labeling experiments were not fully conclusive regarding intracellular Mam12 localization (46). In contrast, the observed localization of MamC-GFP as a bright dot at midcell might indicate that the intracellular localization of the MamC protein along the chain is variable and may change over the cell cycle. The absence of strong fluorescence and immunosignals from different compartments of cells expressing GFP fusions to either MamC, MamF, or MamG indicated that these hydrophobic proteins are targeted exclusively to the MM. This is in contrast to other, more hydrophilic magnetosome proteins, which showed a variable and slightly different subcellular localization. For instance, in *M. magneticum*, GFP fusions of the protein MamA, which is postulated to be involved in the "activation" of magnetite precipitation and the regulation of magnetosome chain length, showed a growth stage-dependent localization pattern. During exponential phase, a filamentous structure was seen, which reached from pole to pole, and stationary cells displayed more punctuated signals at midcell (17). GFP fused to MamK, which is an actin-like protein presumably forming the cytoskeletal magnetosome filament, localized as straight lines that extended through most of the cell (16). Similar to MamK and MamA, GFP fused to the MamJ protein of *M. gryphiswaldense*, which is predicted to attach magnetosome vesicles to the magnetosome filament, localized as long filaments extending from pole to pole (33). While the localization of these hydrophilic proteins clearly extended the length of the magnetosome chains, the linear fluorescent signals corresponding to the MamGFC-GFP fusions seem to be confined to the position of the chain of magnetite crystals. Remarkably, none of the MamGFC-GFP proteins were found to be associated with the cytoplasmic membrane, although MamGFC are hydrophobic proteins with a predicted localization in the cytoplasmic membrane. Hence, our data indicate that MamC, MamF, and MamG are targeted to the MM by a highly specific mechanism that seems different from those of other MMPs, such as MamA, MamJ, and MamK. It is possible that certain MM proteins, such as MamA, MamJ, and MamK, display a localization pattern different from that of MamC, MamF, and MamG, as they interact with the magnetosome filament, whereas MamC, MamF, and MamG, which are part of the MM, are predominantly associated with mature magnetsomes.

The utilization of magnetic nanoparticles for many applications generally requires a specifically functionalized particle surface (reviewed in reference 22). For example, it is very attractive to specifically display foreign polypeptides, such as enzymes, fluorophores, or coupling groups, on the surfaces of particles, and the genetic modification of magnetosome-associated proteins may provide an elegant way to construct multifunctionalized magnetic nanoparticles. In our study, the MamC-GFP fusion protein retained functionality in vitro and remained attached to the magnetosomes after their isolation from disrupted cells, as indicated by robust magnetosome-specific fluorescence under a variety of storage and incubation conditions. Such GFP-coupled magnetosomes might be useful as fluorescence-labeled magnetic nanoparticles in several applications, such as bimodal contrast agents for the fluorescent and magnetic resonance imaging of macrophages (24). In addition to GFP, other functional moieties, such as enzymes, antibody binding proteins, receptors, peptide hormones, growth factors, autobiotinylation signals, and protein tags for "click chemistry," could be expressed on the magnetosome particle by the use of magnetosome-specific anchor proteins. Previous studies with *M. magneticum* attempted to use either the MagA or Mms16 protein as a membrane anchor for magnetosome-specific display of fusion proteins (28, 53). However, the idea that MagA and Mms16 (renamed as ApdA in *M. gryphiswaldense*) are native constituents of the MM has been challenged; in fact, they may rather represent contaminations from other subcellular compartments that become nonspecifically associated with the magnetosome particles upon cell disruption (10, 34, 37). Magnetosomes modified with a luciferase fusion of the magnetosome protein Mms13, which is an ortholog of MamC, had more than 400-fold-higher luminescence intensity than Mms16-luciferase-modified magnetosomes in *M. magneticum* AMB-1 (53). This is in agreement with our results, which demonstrated that GFP fused to MamC displayed strong and stable fluorescence in vitro. MamC seems to represent a useful, perhaps universal, anchor for magnetosome display of other proteins for several reasons. First, MamC is

tightly attached to the magnetite crystal surface, and its association has been shown to be resistant to proteolysis and chemical stress (9). Second, as the most abundant magnetosome protein, it is highly expressed. By densitometric quantification, we roughly estimated the number of MamC-GFP copies per magnetosome particle to be 50 to 100 (data not shown). In addition, as an anchor, MamC is not likely to interfere with the function of the added moiety because of its relatively small size, and its hydrophilic C terminus is accessible for the expression of fusion proteins. Conversely, MamC fusions with heterologous proteins are not expected to interfere with magnetosome formation, as it has been demonstrated that the deletion of MamC had only a minor effect on magnetite synthesis (32).

In conclusion, we established cultivation conditions for the expression of GFP in *M. gryphiswaldense.* Under these growth conditions, it is possible to use GFP as fluorescent tag for subcellular protein localization or as a reporter gene to study gene expression in correlation with magnetite synthesis within the same cell. Furthermore, the use of MamC as an anchor for future functionalization of magnetosomes for biotechnological applications has been demonstrated.

ACKNOWLEDGMENTS

We are grateful to Markus Kador and Michael Boshardt for introducing and giving us access to the flow cytometer. We also thank Torsten Pirch and Kirsten Jung for making the 96-well fluorescence reader available and Theis Stüven from Olympus Deutschland for support regarding fluorescence microscopy.

The project was funded by German Research Foundation grant SPP 1104 and the "Nanobiotechnology" program of the German Federal Ministry of Education and Research.

REFERENCES

1. **Bazylinski, D. A., and R. B. Frankel.** 2004. Magnetosome formation in prokaryotes. Nat. Rev. Microbiol. **2:**217–230.
2. **Bazylinski, D. A., and S. Schübbe.** 2007. Controlled biomineralization by and applications of magnetotactic bacteria. Adv. Appl. Microbiol. **62:**21–62.
3. **Bumann, D., and R. H. Valdivia.** 2007. Identification of host-induced pathogen genes by differential fluorescence induction reporter systems. Nat. Protoc. **2:**770–777.
4. **Ceyhan, B., P. Alhorn, C. Lang, D. Schueler, and C. M. Niemeyer.** 2006. Semi-synthetic biogenic magnetosome nanoparticles for the detection of proteins and nucleic acids. Small **2:**1251.
5. **Cormack, B. P., R. H. Valdivia, and S. Falkow.** 1996. FACS-optimized mutants of the green fluorescent protein (GFP). Gene **173:**33–38.
6. **Elowitz, M. B., A. J. Levine, E. D. Siggia, and P. S. Swain.** 2002. Stochastic gene expression in a single cell. Science **297:**1183–1186.
7. **Gorby, Y. A., T. J. Beveridge, and R. Blakemore.** 1988. Characterization of the bacterial magnetosome membrane. J. Bacteriol. **170:**834–841.
8. **Grünberg, K.** 2005. Biochemische und molekulabiologische Untersuchung der Magnetosomenmembran von *Magnetospirillum gryphiswaldense.* Ph.D. thesis. Universität Bremen, Bremen, Germany.
9. **Grünberg, K., E. C. Müller, A. Otto, R. Reszka, D. Linder, M. Kube, R. Reinhardt, and D. Schüler.** 2004. Biochemical and proteomic analysis of the magnetosome membrane in *Magnetospirillum gryphiswaldense*. Appl. Environ. Microbiol. **70:**1040–1050.
10. **Handrick, R., S. Reinhardt, D. Schultheiss, T. Reichart, D. Schüler, V. Jendrossek, and D. Jendrossek.** 2004. Unraveling the function of the *Rhodospirillum rubrum* activator of polyhydroxybutyrate (PHB) degradation: the activator is a PHB-granule-bound protein (phasin). J. Bacteriol. **186:**2466–2475.
11. **Hansen, M. C., R. J. Palmer, C. Udsen, D. C. White, and S. Molin.** 2001. Assessment of GFP fluorescence in cells of *Streptococcus gordonii* under conditions of low pH and low oxygen concentration. Microbiology **147:**1383–1391.
12. **Heim, R., D. C. Prasher, and R. Y. Tsien.** 1994. Wavelength mutations and posttranslational autoxidation of green fluorescent protein. Proc. Natl. Acad. Sci. USA **91:**12501–12504.
13. **Hergt, R., R. Hiergeist, M. Zeisberger, D. Schüler, U. Heyen, I. Hilger, and W. A. Kaiser.** 2005. Magnetic properties of bacterial magnetosomes as diagnostic and therapeutic tools. J. Magn. Magn. Mat. **293:**80–86.
14. **Heyen, U., and D. Schüler.** 2003. Growth and magnetosome formation by microaerophilic *Magnetospirillum* strains in an oxygen-controlled fermentor. Appl. Microbiol. Biotechnol. **61:**536–544.
15. **Komeili, A.** 2007. Molecular mechanisms of magnetosome formation. Annu. Rev. Biochem. **76:**351–366.
16. **Komeili, A., Z. Li, D. K. Newman, and G. J. Jensen.** 2006. Magnetosomes are cell membrane invaginations organized by the actin-like protein MamK. Science **311:**242–245.
17. **Komeili, A., H. Vali, T. J. Beveridge, and D. Newman.** 2004. Magnetosome vesicles are present prior to magnetite formation and MamA is required for their activation. Proc. Natl. Acad. Sci. USA **101:**3839–3844.
18. **Kovach, M. E., P. H. Elzer, D. S. Hill, G. T. Robertson, M. A. Farris, R. M. Roop II, and K. M. Peterson.** 1995. Four new derivatives of the broad-host-range cloning vector pBBR1MCS, carrying different antibiotic-resistance cassettes. Gene **166:**175–176.
19. **Laemmli, U. K.** 1970. Cleavage of structural proteins during the assembly of the head of bacteriophage T4. Nature **227:**680–685.
20. **Lang, C., and D. Schüler.** 2006. Biogenic nanoparticles: production, characterization, and application of bacterial magnetosome. J. Phys. Condens. Matter **18:**S2815–S2828.
21. **Lang, C., and D. Schüler.** 2006. Biomineralization of magnetosomes in bacteria: nanoparticles with potential applications, p. 107–124. *In* B. Rehm (ed.), Microbial bionanotechnology: biological self-assembly systems and biopolymer-based nanostructures. Horizon Bioscience, Wymondham, United Kingdom.
22. **Lang, C., D. Schüler, and D. Faivre.** 2007. Synthesis of magnetite nanoparticles for bio- and nanotechnology: genetic engineering and biomimetics of bacterial magnetosomes. Macromol. Biosci. **7:**144–151.
23. **Larrainzar, E., F. O'Gara, and J. P. Morrissey.** 2005. Applications of autofluorescent proteins for *in situ* studies in microbial ecology. Annu. Rev. Microbiol. **59:**257–277.
24. **Lisy, M.-R., A. Hartung, C. Lang, D. Schüler, W. Richter, J. R. Reichenbach, W. A. Kaiser, and I. Hilger.** 2007. Fluorescent bacterial magnetic nanoparticles as bimodal contrast agents. Investig. Radiol. **42:**235–241.
25. **Margolin, W.** 2005. FtsZ and the division of prokaryotic cells and organelles. Nat. Rev. Mol. Cell Biol. **6:**862–871.
26. **Matsunaga, T., H. Nakayama, M. Okochi, and H. Takeyama.** 2001. Fluorescent detection of cyanobacterial DNA using bacterial magnetic particles on a MAG-microarray. Biotechnol. Bioeng. **73:**400–405.
27. **Matsunaga, T., T. Suzuki, M. Tanaka, and A. Arakaki.** 2007. Molecular analysis of magnetotactic bacteria and development of functional bacterial magnetic particles for nano-biotechnology. Trends Biotechnol. **25:**182–188.
28. **Matsunaga, T., H. Togo, T. Kikuchi, and T. Tanaka.** 2000. Production of luciferase-magnetic particle complex by recombinant *Magnetospirillum* sp. AMB-1. Biotechnol. Bioeng. **70:**704–709.
29. **Patterson, G. H., S. M. Knobel, W. D. Sharif, S. R. Kain, and D. W. Piston.** 1997. Use of the green fluorescent protein and its mutants in quantitative fluorescence microscopy. Biophys. J. **73:**2782–2790.
30. **Reid, B. G., and G. C. Flynn.** 1997. Chromophore formation in green fluorescent protein. Biochemistry **36:**6786–6791.
31. **Sambrook, J., and D. W. Russel.** 2001. Molecular cloning: a laboratory manual, 3rd ed. Cold Spring Harbor Laboratory Press, Cold Spring Harbor, NY.
32. **Scheffel, A., A. Gärdes, K. Grünberg, G. Wanner, and D. Schüler.** 2007. The major magnetosome proteins MamGFDC are not essential for magnetite biomineralization in *Magnetospirillum gryphiswaldense*, but regulate the size of magnetosome crystals. J. Bacteriol. **190:**377–386.
33. **Scheffel, A., M. Gruska, D. Faivre, A. Linaroudis, P. L. Graumann, J. M. Plitzko, and D. Schüler.** 2006. An acidic protein aligns magnetosomes along a filamentous structure in magnetotactic bacteria. Nature **440:**110–115.
34. **Schüler, D.** 2004. Molecular analysis of a subcellular compartment: the magnetosome membrane in *Magnetospirillum gryphiswaldense*. Arch. Microbiol. **181:**1–7.
35. **Schüler, D., and E. Baeuerlein.** 1998. Dynamics of iron uptake and Fe_3O_4 biomineralization during aerobic and microaerobic growth of *Magnetospirillum gryphiswaldense*. J. Bacteriol. **180:**159–162.
36. **Schüler, D., R. Uhl, and E. Baeuerlein.** 1995. A simple light scattering method to assay magnetism in *Magnetospirillum gryphiswaldense*. FEMS Microbiol. Lett. **132:**139–145.
37. **Schultheiss, D., R. Handrick, D. Jendrossek, M. Hanzlik, and D. Schüler.** 2005. The presumptive magnetosome protein Mms16 is a PHB-granule bounded protein (phasin) in *Magnetospirilum gryphiswaldense*. J. Bacteriol. **187:**2416–2425.
38. **Schultheiss, D., M. Kube, and D. Schüler.** 2004. Inactivation of the flagellin gene *flaA* in *Magnetospirillum gryphiswaldense* results in nonmagnetotactic mutants lacking flagellar filaments. Appl. Environ. Microbiol. **70:**3624–3631.
39. **Schultheiss, D., and D. Schüler.** 2003. Development of a genetic system for *Magnetospirillum gryphiswaldense*. Arch. Microbiol. **179:**89–94.
40. **Simon, R., U. Priefer, and A. Pühler.** 1983. A broad host range mobilisation system for *in vivo* genetic engineering: transposon mutagenesis in Gram-negative bacteria. Bio/Technology **1:**784–791.

41. **Southward, C. M., and M. G. Surette.** 2002. The dynamic microbe: green fluorescent protein brings bacteria to light. Mol. Microbiol. **45:**1191–1196.
42. **Stookey, L. L.** 1970. Ferrozine—a new spectrophotometric reagent for iron. Anal. Chem. **42:**779–781.
43. **Strovas, T. J., L. M. Sauter, X. F. Guo, and M. E. Lidstrom.** 2007. Cell-to-cell heterogeneity in growth rate and gene expression in *Methylobacterium extorquens* AM1. J. Bacteriol. **189:**7127–7133.
44. **Tanaka, M., Y. Okamura, A. Arakaki, T. Tanaka, H. Takeyama, and T. Matsunaga.** 2006. Origin of magnetosome membrane: proteomic analysis of magnetosome membrane and comparison with cytoplasmic membrane. Proteomics **6:**5234–5247.
45. **Tanaka, T., H. Yamasaki, N. Tsujimura, N. Nakamura, and T. Matsunaga.** 1997. Magnetic control of bacterial magnetite-myosin conjugate movement on actin cables. Mater. Sci. Eng. C **5:**121–124.
46. **Taoka, A., R. Asada, H. Sasaki, K. Anzawa, L.-F. Wu, and Y. Fukumori.** 2006. Spatial localizations of Mam22 and Mam12 in the magnetosomes of *Magnetospirillum magnetotacticum*. J. Bacteriol. **188:**3805–3812.
47. **Viollier, E., P. W. Inglett, K. Hunter, A. N. Roychoudhury, and P. Van Cappellen.** 2000. The ferrozine method revisited: Fe(II)/Fe(III) determination in natural waters. Appl. Geochem. **15:**785–790.
48. **Wacker, R., B. Ceyhan, P. Alhorn, D. Schüler, C. Lang, and C. M. Niemeyer.** 2007. Magneto-immuno PCR: a homogeneous immunoassay based on biogenic magnetosome nanoparticles. Biochem. Biophys. Res. Commun. **357:** 391–396.
49. **Wadhams, G. H., A. C. Martin, S. L. Porter, J. R. Maddock, J. C. Mantotta, H. M. King, and J. P. Armitage.** 2002. TlpC, a novel chemotaxis protein in *Rhodobacter sphaeroides*, localizes to a discrete region in the cytoplasm. Mol. Microbiol. **46:**1211–1221.
50. **Yang, C. D., H. Takeyama, T. Tanaka, and T. Matsunaga.** 2001. Effects of growth medium composition, iron sources and atmospheric oxygen concentrations on production of luciferase-bacterial magnetic particle complex by a recombinant *Magnetospirillum magneticum* AMB-1. Enzyme Microbiol. Technol. **29:**13–19.
51. **Yoong, P., R. Schuch, D. Nelson, and V. A. Fischetti.** 2006. PlyPH, a bacteriolytic enzyme with a broad pH range of activity and lytic action against *Bacillus anthracis*. J. Bacteriol. **188:**2711–2714.
52. **Yoshino, T., F. Kato, H. Takeyama, K. Nakai, Y. Yakabe, and T. Matsunaga.** 2005. Development of a novel method for screening of estrogenic compounds using nano-sized bacterial magnetic particles displaying estrogen receptor. Anal. Chim. Acta **532:**105–111.
53. **Yoshino, T., and T. Matsunaga.** 2006. Efficient and stable display of functional proteins on bacterial magnetic particles using Mms13 as a novel anchor molecule. Appl. Environ. Microbiol. **72:**465–471.
54. **Yoshino, T., M. Takahashi, H. Takeyama, Y. Okamura, F. Kato, and T. Matsunaga.** 2004. Assembly of G protein-coupled receptors onto nanosized bacterial magnetic particles using Mms16 as an anchor molecule. Appl. Environ. Microbiol. **70:**2880–2885.
55. **Yoza, B., A. Arakaki, and T. Matsunaga.** 2003. DNA extraction using bacterial magnetic particles modified with hyperbranched polyamidoamine dendrimer. J. Biotechnol. **101:**219–228.
56. **Zhang, C., X. H. Xing, and K. Lou.** 2005. Rapid detection of a GFP-marked *Enterobacter aerogenes* under anaerobic conditions by aerobic fluorescence recovery. FEMS Microbiol. Lett. **249:**211–218.